Title
31P NMR CHEMICAL SHIELDING TENSORS OF o-CagP2

Author
Kohler, Susan J.

Publication Date
1976

Submitted to Journal of Chemical Physics

LBL-4698
Preprint

^{31}P NMR CHEMICAL SHIELDING TENSORS OF α-$Ca_2P_2O_7$

Susan J. Kohler, J. David Ellett, Jr., and Melvin P. Klein

January 1976

Prepared for the U. S. Energy Research and
Development Administration under Contract W-7405-ENG-48

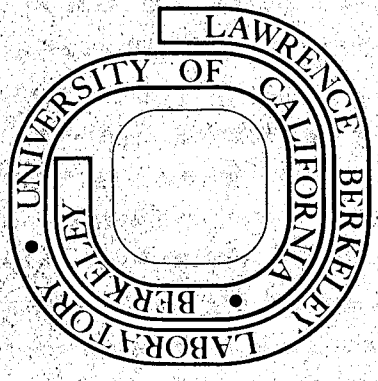

DISCLAIMER

^{31}P NMR Chemical Shielding Tensors of α-$Ca_2P_2O_7$*

Susan J. Kohler†, J. David Ellett, Jr.+, and Melvin P. Klein

Laboratory of Chemical Biodynamics

University of California

Berkeley, California 94720

* Portions of this paper are derived from the dissertation of S.J.K. presented in partial fulfillment of the requirements for a Ph.D. degree, University of California (1975). This research was supported in part by the U. S. Energy Research and Development Administration.

† S.J.K. is a Postdoctoral Fellow of the National Cancer Institute of the National Institutes of Health, grant number 1 F22 CA02169-01.

+ Present address: Pennie, Edmonds, Attorneys at Law, 330 Madison Ave., New York, New York.

ABSTRACT

The ^{31}P NMR chemical shielding tensors were measured in a crystal of α-$Ca_2P_2O_7$; the principal values, relative to 85% H_3PO_4 were found to be -42, 32, 65 ppm for P(1) and -48, 44, 67 ppm for P(2) with an average relative standard deviation of 7%. The most probable orientations of the tensors in the molecule were determined, and in both cases the most downfield component of the shielding tensor is along the P-O(P) bond direction; this orientation is correlated with the electronic distribution around the phosphorous nuclei. The high resolution spectra used in determining the shielding tensors were taken using the multiple pulse WAHUHA technique which removes homonuclear dipolar interactions in solids [J. S. Waugh, L. M. Huber, and U. Haeberlin, Phys. Rev. Let. 20, 180 (1968)]. The linewidths were reduced from 1 KHz to 100 Hz by this technique. Details of the spectrometer design and the tuneup procedure for the WAHUHA experiment are also given.

I. INTRODUCTION

Nuclear magnetic resonance (NMR) has gained widespread use as a spectroscopic probe of the structure and dynamics of molecules in liquids. Analysis of chemical shift data and relaxation time data yields information about the chemical environment of a given nucleus as well as the motion of that nucleus. NMR of solids and of large molecules in solution has in general not been as fruitful due to the large amount of line broadening which obscures the chemical shift information. The line broadening is caused primarily by non-vanishing dipolar interactions which are averaged to zero in solutions where the molecules are tumbling isotropically. Recently developed multiple pulse NMR experiments will remove both the homonuclear[1,2] and heteronuclear[3] dipolar interactions in solids, creating narrow lines and allowing the resolution of the chemical shifts. Since the chemical shift is a second rank tensor, all six components of its symmetric part are obtainable if single crystals are studied.[4,5] This gives potentially six times the information available from a solution spectrum.

^{31}P NMR spectra of the phospholipids in biological membranes and in phospholipid/water dispersions have shown the presence of unresolved dipolar interactions,[6,7] indicating that these systems might benefit from multiple pulse experiments. Interest in these systems has led us to develop a spectrometer capable of performing ^{31}P multiple pulse experiments, and to initiate a study of the chemical shielding tensors of phosphates related to the phospholipid phosphates. The compound α-$Ca_2P_2O_7$ was chosen as the first sample because only homonuclear interactions are present and a simple WAHUHA experiment[1] should suffice to remove the dipolar coupling. In this paper chemical shielding tensors of α-$Ca_2P_2O_7$ are reported.

II. THEORETICAL

In the WAHUHA experiment[1] a cyclic application of radio frequency (rf) pulses applied along the $\pm x$ and $\pm y$ directions in the rotating frame causes the average dipolar interaction to vanish when the system is sampled at the appropriate times. The disappearance of the dipolar interaction can be explained in terms of average hamiltonian theory which is well understood[8,9] and will be only briefly described here. If we consider a system of like nuclei in a magnetic field which are subjected to radiofrequency irradiation, the hamiltonian operator in the rotating Zeeman frame can be written

$$\mathcal{H}(t) = \mathcal{H}_{int} + \mathcal{H}_{rf}(t)$$

where $\mathcal{H}_{rf}$ is due to the radiofrequency and $\mathcal{H}_{int}$ contains internal interactions such as dipolar coupling, chemical shift, and J-coupling appropriate to the specific system. This hamiltonian may be transformed to a more convenient dynamic reference frame where explicit time dependence is removed from $\mathcal{H}$. The nature of this reference frame depends on the nature of the rf perturbation. If the rf perturbation is cyclic with a period short compared to the normal relaxation times, the hamiltonian may be averaged over the period of the rf cycle and a new average hamiltonian written in terms of a Magnus series expansion.[8] This hamiltonian describes the behavior of the system when it is observed in a periodic fashion, i.e., once/rf cycle. $\mathcal{H}_{int}$ contains terms which are spherical tensors of various ranks. Since spherical tensors of different ranks behave differently under transformation, the final average terms will have different forms. Thus rf cycles may be designed to affect different parts of the nuclear spin interaction. In the specific case of the four-pulse WAHUHA experiment in the limit of δ-function pulses, the chemical shift term is scaled by $1/\sqrt{3}$ and the homonuclear dipolar interaction is reduced to zero.[8]

When the dipolar interactions are removed, the chemical shifts of the nuclei are revealed. In the case of a powder sample containing randomly distributed crystallites, the spectrum assumes a characteristic powder pattern,[10] and the principal values of the shielding tensor may be read directly from the spectrum. When the sample is a single crystal, narrow resonances are observed. Their number depends on the symmetry of the unit cell and on the number of chemically inequivalent nuclei in the asymmetric unit. Their frequencies ω depend on the orientation of the crystal with respect to the magnetic field according to the equation

$$\omega = \omega_o(1-\sigma_{zz})$$

with

$$\sigma_{zz} = \sum_{i,j} r_{zi}\, r_{zj}\, \sigma^c_{ij} \qquad (1)$$

where σ_{zz} is the measured chemical shift, r_{zi} and r_{zj} are direction cosines between the z laboratory axis and the i^{th} and j^{th} crystal axes, and the superscript c indicates a crystal-based reference frame. If the crystal is rotated about an axis perpendicular to the magnetic field direction and the resonance frequency is measured as a function of rotation angle, three components of the shielding tensor in the crystal-based reference frame are obtained. If this process is carried out for three different orientations of the crystal, all the components of the symmetric part of the chemical shielding tensor in the crystal frame are obtained. This tensor is most useful if it can then be related to the orientation of the molecule, as is formally written

$$\sigma^c_{ij} = \sum_{\alpha\beta} r_{i\alpha}\, r_{j\beta}\, \sigma^m_{\alpha\beta} \qquad (2)$$

where $r_{i\alpha}$ and $r_{j\beta}$ are direction cosines between the i,j crystal axes and the α, β molecular axes and the superscript m refers to a convenient molecular reference frame. Experimentally this is accomplished by using x-ray

crystallography to determine the orientation of the molecular frame with respect to the crystal-based (c) frame.

III. EXPERIMENTAL METHODS

The WAHUHA experiments were done in a homebuilt double resonance spectrometer incorporating a Varian 14 kgauss magnet. The spectrometer, diag ammed in Figure 1, operates with four phases of radiofrequency (rf) at the phosphorous resonance frequency of 24.3 MHz, has 60 MHz available at high power levels for proton irradiation, and is further equipped with an external deuterium field-frequency lock operating at 9.21 MHz. Although the 60 MHz capabilities were not used in the α-$Ca_2P_2O_7$ experiments, they will be described for the sake of completeness. In addition to the spectrometer, the experimental apparatus includes an automated goniometer and computer-driven goniometer controller for positioning the sample. Data acquisition and control of the experiment were performed by a Nicolet NIC-80 computer. The more specialized features of the spectrometer and the physical setup will be described in this section.

FIG. 1

A. Spectrometer

1. Probe Circuits

The WAHUHA experiment requires a probe circuit which will transmit high levels of rf power to the sample, recover rapidly from rf pulses, and detect low level signals from the sample. These requirements are met by the circuit shown in Figure 2a. Impedance matching of the transmitter to the resonant circuit insures efficient power transfer. The crossed diodes at the end of the $\lambda/4$ cable switch the 50 Ω load in and out of the effective circuit, making it low Q (fast recovery) when in the transmitter mode and high Q (high sensitivity) when in the receiver mode. The sensitivity of the system was such that the free induction decay of approximately 150 mg K_2HPO_4 powder could

FIG. 2

be seen in one pass. The strength of the magnetic field produced in the coil was approximately 100 gauss when operating at a power of 1 kwatt.

The design of the 60 MHz circuit was not as critical as that of the 24.3 MHz circuit since rapid recovery from pulses was not a requirement. A simple parallel resonant circuit was impedance matched to the transmitter and receiver as shown in Figure 2b. The crossed diodes are used to switch between the transmitter and receiver modes, as is common practice for single coil circuits. One feature of this circuit was the use of a multiple turn Helmholz coil wound of copper ribbon and insulated with Teflon between the turns. The multiple turns increase the field produced at the sample, and the use of ribbon provides lower inductance per length and enables the coil to withstand the high rf levels. The field produced in the sample with this arrangement was approximately 18 gauss when operating at a power of 3.6 kwatt. Details of the physical arrangement of the coils in the probe are shown in Figure 3.

FIG. 3 →

2. 24.3 MHz Transmitter and Receiver

A Hewlett-Packard frequency synthesizer supplies the basic 24.3 MHz rf for the spectrometer. This rf signal passes immediately into a Merrimac quadripolar phase shifter which divides the rf into four signals having nominally the four quadrature phases (0°, 90°, 180°, 270°). The phases are precisely adjustable to within 0.1 degree over a range of at least 30° about their nominal value. The four rf signals are routed into four channels which are separately gated by externally applied logic pulses. The resulting rf pulses are recombined in a Merrimac power combiner and appear on a single output line. The pulses are amplified in a Bruker high power amplifier and then are sent to the probe.

The signal received from the probe is fed through a low noise 24.3 MHz preamp described in detail elsewhere.[11] A string of 16 pairs of crossed

1N914 diodes to ground precede the preamp to protect it from the rf pulses from the transmitter. Even with the diodes, some rf from the transmitter reaches the preamp where it is amplified to a level capable of saturating the later stages of the receiver system. This problem is eliminated by gating off the 30 MHz reference to the linear IF converter while the pulses are on. With this arrangement, the receiver system recovers rapidly and is capable of taking data approximately 10 microseconds after the end of a rf pulse.

The signal from the preamp is transmitted to the linear converter which converts the 24.3 MHz to 60 MHz. It is then phase detected and further amplified. The signal is next fed to an integrate-and-hold circuit, and then to the computer's A-to-D converter. The integrate-and-hold circuit uses an Analog Devices 48 K op amp as the integrator; it is otherwise similar to the circuit described by Ellett et al.[12]

3. 60 MHz Transmitter

The initial 60 MHz rf passes through a switched 90° phase shifter employing a quadrature hybrid. The rf is then gated with a Relcom rf switch controlled by logic from the computer. The rf pulses are amplified by an RF communications 805 which drives a homebuilt 10 kwatt amplifier which feeds the probe.

4. Pulse Programming Network

The Nicolet computer operating with a modified version of the Nicolet T1PRGM is used to supply the initial logic for the generation of rf pulses, receiver gate, and address advance pulses, and also to process the final data. The computer runs in conjunction with a Nicolet 293 I/O Controller containing a series of digital timers which produce logic pulses whose lengths are set by times loaded in from the computer, and whose sequences are determined by the connections of the timers as controlled by the wiring of a patch panel.

The pulses from the Nicolet 293 pass through external driver amplifiers and are then used as the appropriate gates. For a WAHUHA experiment, the pulses go to a two-count pulse sorter which distinguishes between two subcycles of pulses and sends out triggers to a four-pulse generator and to the receiver gate and integrate-and-hold at the appropriate times. The four-pulse generator uses ganged one-shots to produce logic pulses of highly accurate lengths.[12] The lengths of the pulses are individually set, and are also controlled by a fine master trim which adjusts all four pulse lengths simultaneously.[13] These logic pulses gate the four channels from the quadripolar phase shifter, and therefore determine the lengths of the rf pulses.

5. Goniometer and Magnet

The single crystal experiments require that the crystal be rotated about an axis perpendicular to the magnetic field direction. This is accomplished through the use of a specially designed Supper goniometer driven by a Superior Electric Slo-Syn stepping motor. The chief component of the goniometer is a vertical shaft which is turned by a long horizontal shaft extending to the gears of the stepping motor placed outside the magnetic field. The sample is mounted on a rod fitting into a chuck on a mounting head, which is in turn attached to the vertical goniometer shaft. The mounting head was designed to match the standard x-ray crystallographic goniometer heads and therefore allows mounting the sample directly on x-ray crystallographic equipment as well. Since the goniometer must be placed inside the magnetic field, it was constructed entirely of non-ferromagnetic materials.

The HS-25 stepping motor is run by a Harshaw model XC-11 goniometer controller interfaced to the Nicolet computer. The goniometer and controller were designed to control the sample orientation to within 0.01 degrees. The reproducibility of this system was demonstrated by noting that a spectrum taken at a given orientation would be reproduced exactly after the crystal

was rotated away and then returned to the initial angle.

In order to create a larger working area to mount the goniometer above the probe, the 14 kgauss magnet was rotated 45° from the vertical. The shim coils were rotated back to their original positions to maintain the shim Y axis as the vertical direction. Two sets of vertical rods mounted on the tilted magnet hold Bruker probe holders into which are placed the probe and goniometer.

B. Tuneup of WAHUHA Experiment

The WAHUHA experiment is extremely sensitive to proper pulse lengths and phases, and the presence of phase transients. A combination of the methods of Vaughan[2] and Waugh[12] was used for the tuneup procedure.

A sample of 85% H_3PO_4 solution was placed in the probe and the exact resonance frequency was found. The Bruker amplifier was tuned to give a square rf pulse when sampled at the 50 Ω load, and the probe was tuned to give maximum signal amplitude for the H_3PO_4 free induction decay. The four rf phases were set with the use of a Hewlett-Packard 8405A vector voltmeter. The 90° pulse lengths for each of the four phases were set using the train of 90° pulses shown in Figure 4a. While irradiating the sample with the train

Fig 4 →

of pulses, the pulse length was adjusted until the pattern of Figure 4b was obtained, indicating proper setting of the 90° length. Using the phase alternated sequence of Figure 4c, the tuning of the Bruker amplifier was adjusted so that no beats were seen in the signal with the spectrometer on resonance, and the beat frequencies were the same for equal frequency offsets above and below resonance. This procedure minimizes the phase transient effects. The pulse lengths were then rechecked using the first sequence described above. The full WAHUHA sequence was used with H_3PO_4 at exact resonance and the pulse lengths and phases were carefully adjusted until the beats in the decay were removed. As a final check, a plot was made of the apparent chemical shift as a function of resonance offset. Theory

predicts that such a plot should be linear and pass through the origin. For the case of 2 μsec pulses and a 50 μsec cycle time, the slope is calculated to be 0.60.[8] These parameters were used as the criteria for proper tuning.

C. Preparation of Sample

α-$Ca_2P_2O_7$ doped with Mn^{2+} was the gift of Professor Alex Pines of the University of California, Berkeley, and it originally came from the laboratory of Professor C. Calvo at McMaster University. The lengths of the unit cell axes were measured and found to be a = 12.61 A^o, b = 8.51 A^o, and c = 5.26 A^o, in good agreement with the reported values of 12.66, 8.54, and 5.315 A^o.[14] The orientation of the unit cell of the crystal was determined by the Laue precession method and a crystal-based reference frame was defined by three glass plates which were glued to the crystal. Each time the mounting of the crystal was changed for a new rotation study, the orientations of the glass plates were measured with an optical goniometer and the orientation of the crystal reference frame was thus determined. These orientations were measured before and after each NMR run, and found to be reproducible to within 1 degree.

IV. RESULTS

A. Effectiveness of the WAHUHA Experiment

The WAHUHA experiment is highly effective in removing phosphorous homonuclear broadening in solids. This is illustrated by the spectra of α-$Ca_2P_2O_7$ shown in Figure 5. Spectrum (a) is from a typical free induction decay (FID) experiment with a digitizing rate of 10 μsec per point. Spectrum (b) is from a 4-pulse WAHUHA experiment with 2 μsec pulses and a 48 μsec cycle time performed on the same sample in the same orientation. The scaling of the chemical shifts by approximately $1/\sqrt{3}$ is clearly evident. The line width of approximately 1 KHz seen in the free induction decay experiment is reduced to 100 Hz by the WAHUHA experiment. Additional experiments have shown a further reduction

FIG 5 →

in linewidth with the use of more sophisticated cycles such as the 8-pulse WAHUHA[8] or REV-8 cycles[15] which compensate for imperfections in the four pulse WAHUHA cycle and cause higher order terms in the dipolar interaction to vanish. For example, the REV-8 experiment done with 2 μsec pulses and a 114 μsec cycle time reduced the line widths by an additional factor of 1/3 to 1/2 from the 80-200 Hz widths seen in a 4-pulse WAHUHA experiment. When using the REV-8 cycle, the peaks all had approximately the same widths. This is in contrast to the 4-pulse WAHUHA experiment where the peaks further from the pulsing frequency were broader.

B. α-$Ca_2P_2O_7$ Chemical Shielding Tensor

WAHUHA spectra were taken as a function of rotation angle for three different initial orientations of a crystal of α-$Ca_2P_2O_7$. The spectra were taken in 5° intervals over a range of 180°. A typical spectrum shown in Figure 6 was taken with 2 μsec pulses and a 56.4 μsec cycle time and contains 400 passes taken at the rate of one every 15 seconds. The pulsing frequency was 24.284 MHz, approximately 3.3 KHz above the H_3PO_4 resonance frequency.

FIG. 6 →

Knowledge of the Laue point group and number of resonant nuclei per asymmetric unit allows the prediction of the maximum number of lines which may be seen at any orientation of the crystal.[16] Specifically, α-$Ca_2P_2O_7$ crystallizes in the monoclinic space group $P2_1/n$ (Laue point group 2/m) and has one molecule per asymmetric unit.[14] There are therefore four molecules per unit cell, occurring in two pairs related by inversion symmetry. Since shielding tensors are invariant under inversion, the chemical shifts from the members of each pair are identical, and only two molecules will be distinguishable in NMR spectra. Each molecule has two phosphorous nuclei, and therefore a maximum of four lines is predicted for a ^{31}P NMR spectrum of α-$Ca_2P_2O_7$, as seen in Figure 5. However, eight distinct lines are seen in the spectra of the α-$Ca_2P_2O_7$ crystal used for the tensor determinations. The fact

that exactly twice the predicted number of lines are seen indicates that this crystal is twinned. This is not surprising, since twinning about the c axis is common for α-$Ca_2P_2O_7$.[17] The unit cells of such twins are related by a 180° rotation about the c axis, rotating the b axis into the -b direction and the a axis back into the ac plane.

The resonance positions as a function of rotation angle were measured and fitted to equation (1) with a least squares program. The experimental points and theoretical curves are shown in Figure 7. The full tensors are found from the sets of corresponding curves from each of the three rotation plots. For each pair of rotation plots there are points of equivalent orientation as shown by the vertical lines in Figure 7. Comparison of the spectra taken at three equivalent orientations permitted identification of the sets of corresponding peaks and these correspondences were confirmed as the cases with lowest variance when all 512 possible curve combinations were tried with the full tensor least squares fit.

FIG 7 →

Once the eight tensors had been determined, the problem of assigning them to the appropriate phosphorous nuclei remained. Two chemically equivalent nuclei on symmetry-related molecules in a crystal will have congruent shielding tensors having the same principal values but differing in orientation. There is no *a priori* method for determining which tensor corresponds to which molecular orientation. In addition, the presence of two chemically different nuclei in the unit cell creates the further problem of determining which of the two incongruent tensors is associated with each nucleus. Thus the tensor assignment is not unique, and must rely on chemical intuition.

The eight tensors were divided into two groups of congruent tensors, where the members of a group were related by screw symmetry about the crystallographic b axis (the symmetry imposed by the $P2_1/n$ space group) and by a 180° rotation about the c axis (the symmetry imposed by the twinning). The possible tensor

orientations on the pyrophosphate ion were then plotted using ORTEP[a], and only the one shown in Figure 8 showed any obvious correlation with the structure of the ion.

FIG 8 →

The eigenvalues of these tensors and their screw-related counterparts for each crystallite were corrected for the 0.60 scale factor and are reported in Table II. The differences within the sets of values reported for P(1) and for P(2)[b] are an indication of the experimental error in the determinations since the congruent tensors should have identical eigenvalues. It is not understood why the values for P(1) have such a large spread compared with those of P(2), since all tensors were obtained simultaneously under the same experimental conditions. The difference between the average values of σ_{22} for P(1) and P(2) are significant and might be attributed to the small differences in the geometry of the two halves of the pyrophosphate anion, indicating that the shielding tensor is an extremely sensitive probe of environment.

TABLE II →

V. DISCUSSION

In general, the chemical shielding tensors depend on the electronic distributions in both the ground and excited states of the molecule.[18] This makes chemical shielding parameters quite difficult to calculate quantitatively. However, we have observed that the orientations of the ^{31}P chemical shielding tensors of α-$Ca_2P_2O_7$ correlate simply with the electron distribution found in the ground state of the molecule. Similar correlations have been observed for the ^{31}P chemical shielding tensors of phosphorylethanolamine[19] and $CaHPO_4 \cdot 2H_2O$.[20] These compounds all contain PO_4 units but differ in the degree to which the PO_4

---

[a] ORTEP is the Oak Ridge Thermal Ellipsoid Plot program commonly used to plot crystallographic unit cells.

[b] P(1) and P(2) refer to the two phosphorous atoms as numbered in the original x-ray crystallographic report.[14]

is perturbed by further bonding. The PO_4^{3-} ion itself is a regular tetrahedron, having P-O bond lengths which are all approximately 1.54 A°. This value is less than the calculated single P-O bond length of 1.71 A°[21] indicating some double bond character. The partial double bond character of all the bonds in PO_4^{3-} has been explained in terms of bonding between the empty $3d_{z^2}$ and $3d_{x^2-y^2}$ orbitals of the phosphorous and the filled 2p and 2p' orbitals of the oxygens.[22] When the ion is perturbed by protonation or esterification, bonding will involve one of the 2p orbitals of the participating oxygen, thus reducing the participation of that orbital in π bonding with the phosphorous atom. The resulting effect is that the double bond character of the P-O(R) bond is reduced and the double bond character of the bonds to the non-esterified oxygens is increased. This shifts the electron density away from the P-O(R) bond and toward the remaining P-O bonds, lengthening the former and shortening the latter. The effects of forming a (P)O-H bond are similar to those of forming a (P)O-R bond, although the magnitude of the perturbation is smaller. As an example, serine phosphate has its (R)O-P bond lengthened to 1.61 A°, the (H)O-P bond lengthened to 1.56 A°, and the remaining P-O bonds shortened to 1.52 and 1.50 A°.[22,23]

The bond lengths and bond angles for α-$Ca_2P_2O_7$ are found in Table III. TABLE III → The pyrophosphate anion may be considered to be a phosphate ester where the bridge oxygen has only one 2p orbital available for π bonding with the two phosphorous atoms. Therefore the P-O(P) bond lengths are longer than those of a PO_4^{3-} ion, and the remaining P-O bonds are shorter. The longer bonds with less π character will have a lower electron density and it therefore might be expected that the phosphorous nucleus will be deshielded along the P-O(P) direction. It was observed that the most downfield component of the shielding tensor lies along the unique P-O(P) direction and is therefore in the direction of lowest electron density. Similar correlations were observed for phosphorylethanolamine and $CaHPO_4 \cdot 2H_2O$, where the most downfield components of the shielding tensors were in the planes defined by the bonds of lowest electron

density and the most upfield components were in the planes of highest electron density of the molecular ground states.

ACKNOWLEDGEMENTS

The authors thank Dr. L. Brown for orienting the α-$Ca_2P_2O_7$ crystal and Dr. A. Zalkin for a helpful discussion of crystal twinning.

Table I: Initial Orientations of the α-$Ca_2P_2O_7$ Crystal for the Three Rotations[a]

		ϕ[b]	θ[c]
Rotation I.	a^*	-16.2	75.0°
	b^*	-7.7	165.9
	c^*	74.4	87.8
Rotation II.	a^*	270.4	131.4
	b^*	173.3	98.0
	c^*	74.5	137.5
Rotation III.	a^*	58.4	143.9
	b^*	161.2	99.2
	c^*	77.6	55.5

[a] a^*, b^*, and c^* are the reciprocal axes of the crystal unit cell.

[b] ϕ is the angle from the magnetic field direction (Z) to the projection of the reciprocal axis in the X-Z plane.

[c] θ is the azimuthal angle from the rotation axis (Y) to the reciprocal axis.

Table II: Principal Values of the ^{31}P Chemical Shielding Tensors of α-$Ca_2P_2O_7$[a]

	σ_{11}	σ_{22}	σ_{33}
P(1)[b]	-48	34	73
	-44	31	68
	-43	33	65
	-32	32	54
Average[c]	-42	32	65
P(2)	-44	44	66
	-49	44	68
	-50	45	68
	-48	45	66
Average	-48	44.5	67

[a] All values in ppm relative to H_3PO_4, taking resonances at lower field as negative.

[b] P(1) and P(2) refer to the two phosphorous nuclei as numbered in the original x-ray crystallographic work.[14]

[c] This is a simple numerical average of the four values listed.

Table III: Structure Data for α-$Ca_2P_2O_7$[a]

Bond Lengths		Bond Angles	
P(1)-O(1)	1.579 A°	O(1)-P(1)-O(3)	110.5°
P(1)-O(3)	1.517	O(1)-P(1)-O(5)	109.7
P(1)-O(5)	1.554	O(1)-P(1)-O(7)	105.3
P(1)-O(7)	1.505		
P(2)-O(1)	1.616	O(1)-P(2)-O(2)	107.9°
P(2)-O(2)	1.538	O(1)-P(2)-O(4)	109.2
P(2)-O(4)	1.505	O(1)-P(2)-O(6)	106.4
P(2)-O(6)	1.493		
		P(1)-O(1)-P(2)	130.0

[a] Data from Ref. 14.

FIGURE CAPTIONS

Figure 1. Block diagram of the double resonance spectrometer. The spectrometer operates with four phases of 24.3 MHz for ^{31}P resonance and at 60 MHz for ^{1}H decoupling. The spectrometer is shown in a configuration to perform a WAHUHA experiment. All logic paths are represented by dashed lines, and the rf paths appear as solid lines.

Figure 2. 24.3 MHz and 60 MHz probe circuits.
a) The 24.3 MHz circuit.
b) The 60 MHz circuit.

Figure 3. Central area of probe. The 25 mm long 24.3 MHz coil is wound on the inside of a 10 mm ID glass tube suspended in the cylindrical dewar. Over the glass tube is fitted a Teflon sleeve on which the 60 MHz coil is wound. The coil is a multiple turn Helmholz coil oriented perpendicular to the 14 kgauss magnetic field. The leads from the coils are insulated with Teflon and Mylar and pass out of the central chamber to the capacitors. The probe is designed to pass cooling gas up through the glass tube past the sample, then down the outside of the tube and out through the bottom.

Figure 4. Pulse sequences used in tuning WAHUHA experiment. a) $\pi/2$ pulse train. Each pulse is a $\pi/2$ pulse about the X axis in the rotating reference frame. b) Signal seen from the pulse sequence of (a) with the pulse spacing 50 μsec. The horizontal scale is 500 μsec/division. c) Phase alternated $\pi/2$ pulse train. Each pulse is a $\pi/2$ pulse about the X or -X axis in the rotating reference frame.

Figure 5. 24.3 MHz NMR spectra of α-$Ca_2P_2O_7$. a) Spectrum from a free induction decay experiment of a single crystal of α-$Ca_2P_2O_7$. The digitizing rate was 10 μsec/pt, and 25 passes were accumulated. b) Spectrum from a 4-pulse WAHUHA experiment. The sample is the same as in (a), and the orientation is the same. This experiment was done with 2 μsec pulses and a cycle time of 48 μsec and is the accumulation of 100 passes. The frequency scale applies to both spectra.

Figure 6. Typical WAHUHA spectrum of the α-$Ca_2P_2O_7$ sample used to obtain the shielding tensor. The WAHUHA experiment was done with 2 μsec pulses and a cycle time of 56.4 μsec. This spectrum contains 400 passes accumulated at a rate of one per 30 sec. The scale is in ppm relative to 85% H_3PO_4 using the convention that higher field positions are positive. The scale has been compensated for the approximate $1/\sqrt{3}$ WAHUHA scaling factor.

Figure 7. Angular dependence of ^{31}P resonance frequencies for three different rotations of an α-$Ca_2P_2O_7$ crystal. These plots include data points and theoretical curves calculated from least squares analyses. The vertical lines locate equivalent sample orientations, as indicated by the labels A, B, C. The initial orientations of the crystallographic axes for each rotation are given in Table I.

TABLE I →

Figure 8. Chemical shielding tensor of α-$Ca_2P_2O_7$. These are projections of the molecule in the principal axis system of the shielding tensor of P(1). The shielding tensors are shown as ellipsoids with the shortest axis representing the most downfield tensor component. The numbering of the atoms corresponds to that of the original x-ray crystallography.[14]

REFERENCES

1. J. S. Waugh, L. M. Huber, and U. Haeberlen, Phys. Rev. Let. 20, 180 (1968).
2. W.-K. Rhim, D. D. Elleman, and R. W. Vaughan, J. Chem. Phys. 59, 3740 (1973).
3. A. Pines, M. G. Gibby, and J. S. Waugh, J. Chem. Phys. 59, 569 (1973).
4. R. G. Griffin, J. D. Ellett, M. Mehring, J. G. Bullitt, and J. S. Waugh, J. Chem. Phys. 57, 2147 (1972).
5. M. G. Gibby, A. Pines, W.-K. Rhim, and J. S. Waugh, J. Chem. Phys. 56, 991 (1972).
6. D. G. Davis and G. Inesi, Biochim. Biophys. Acta 282, 180 (1972).
7. A. F. Horwitz and M. P. Klein, J. Supramol. Struct. 1, 19 (1972).
8. U. Haeberlen and J. S. Waugh, Phys. Rev. 175, 453 (1968).
9. M. Mehring and J. S. Waugh, Phys. Rev. B: 5, 3459 (1972).
10. N. Bloembergen and T. J. Rowland, Phys. Rev. 97, 1679 (1957).
11. B. Leskovar, Nucl. Instrum. Methods 47, 29 (1967).
12. J. D. Ellett, M. G. Gibby, U. Haeberlen, L. M. Huber, M. Mehring, A. Pines, and J. S. Waugh, Adv. Magn. Reson. 5, 117 (1971).
13. R. W. Vaughan, private communication.
14. C. Calvo, Inorg. Chem. 7, 1345 (1968).
15. W.-K. Rhim, D. D. Elleman, and R. W. Vaughan, J. Chem. Phys. 58, 1772 (1973).
16. J. A. Weil, T. Buch, and J. E. Clapp, Adv. Magn. Reson. 6, 183 (1973).
17. J. R. Lehr, E. H. Brown, A. W. Frazier, J. P. Smith, and R. D. Thrasher, eds., Crystallographic Properties of Fertilizer Compounds, National Fertilizer Development Center, Muscle Shoals, Alabama, 83 (1967).
18. N. F. Ramsey, Phys. Rev. 86, 243 (1952).
19. S. J. Kohler and M. P. Klein, Biochemistry, in press.
20. S. J. Kohler, unpublished data.
21. V. Shomaker and D. P. Stevenson, J. Amer. Chem. Soc. 63, 37 (1941).
22. D. W. J. Cruickshank, J. Chem. Soc. 1961, 5486 (1961).
23. G. H. McCallum, J. M. Robertson, and G. A. Sim, Nature 184, 1863 (1959).

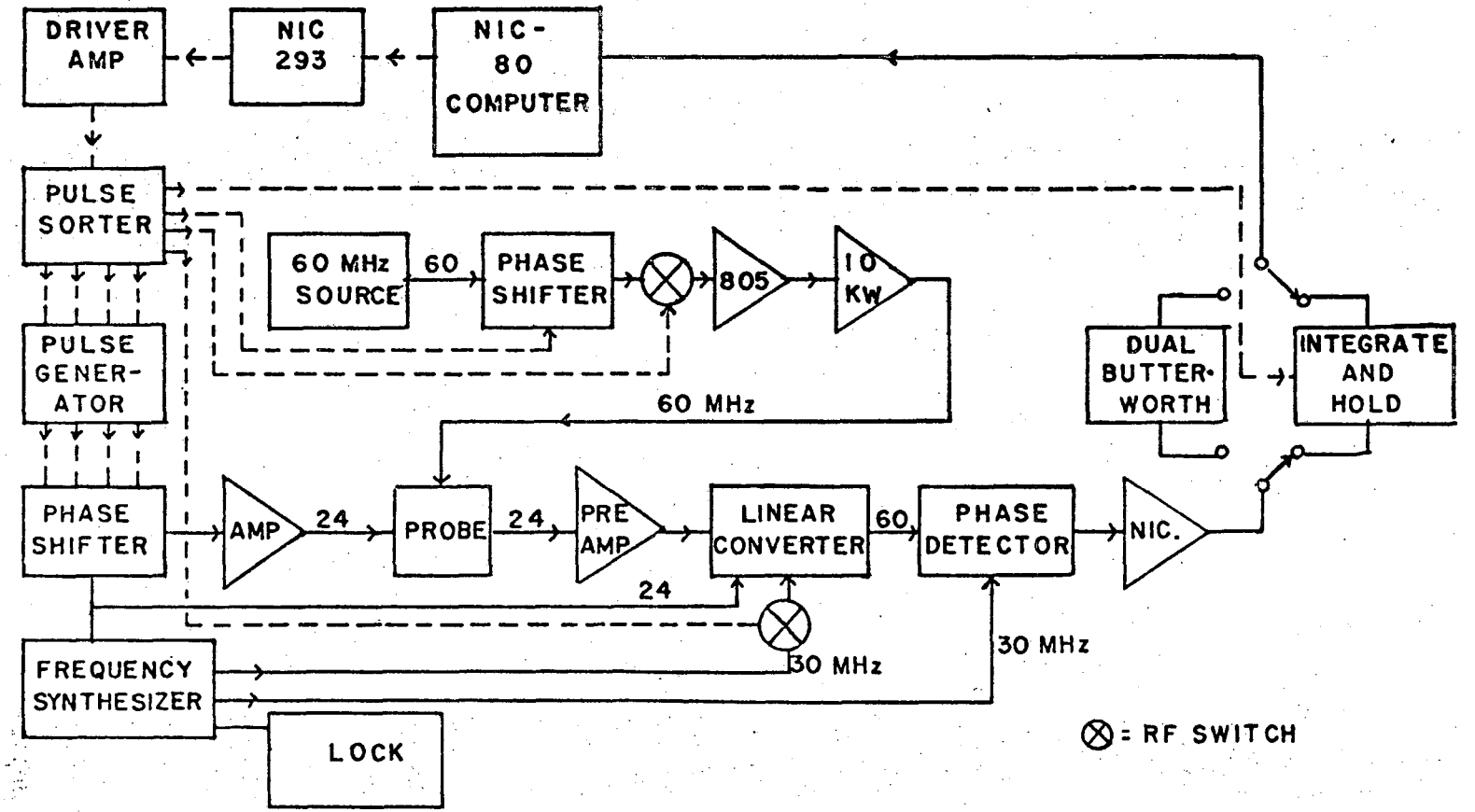

XBL762-5664

Kohler et. al.

FIG 1

a) 24.3 MHz

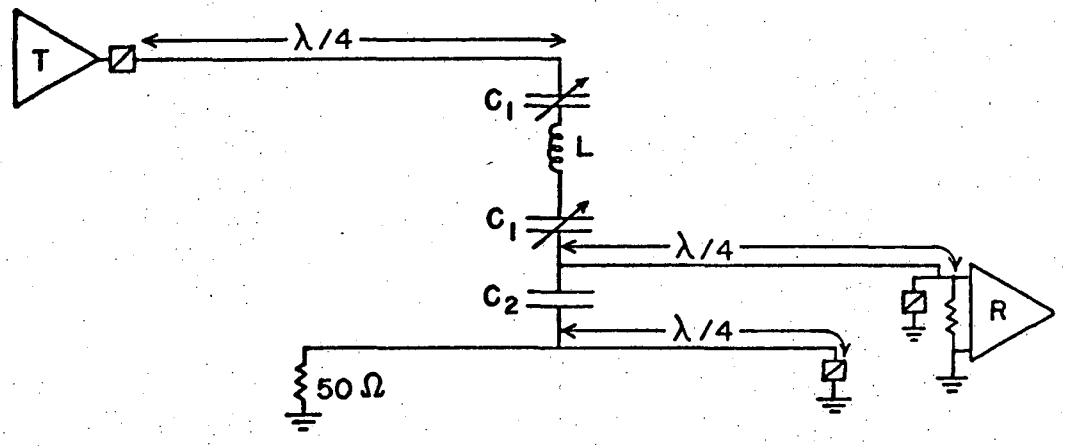

b) 60 MHz

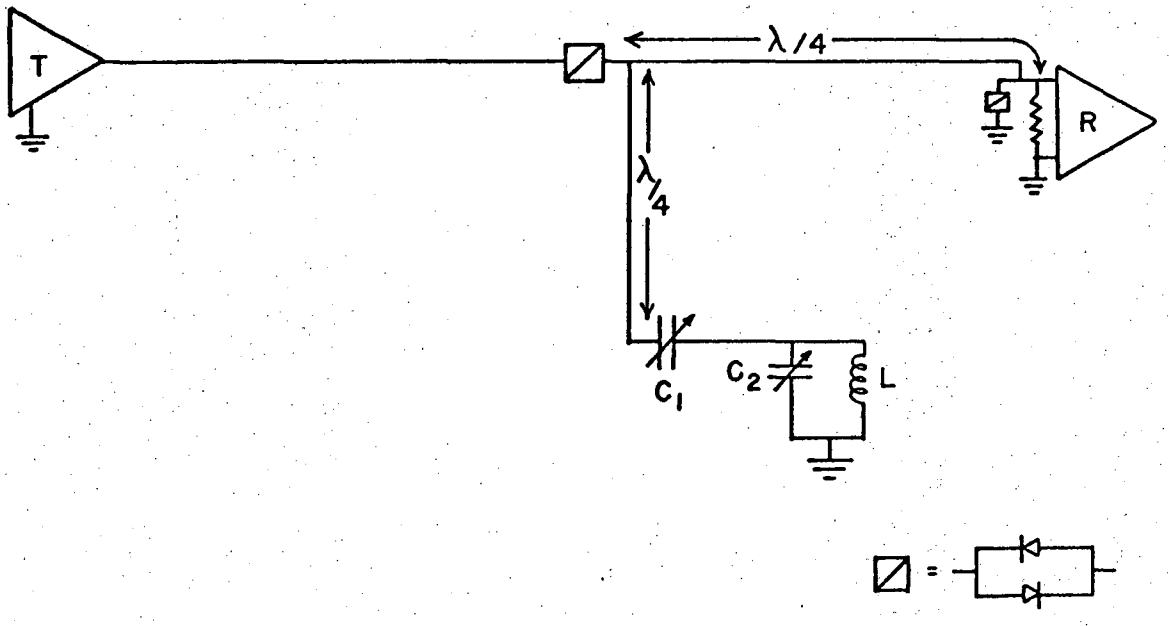

XBL7511-8742

Kohler et al.

FIGURE 2 jcf

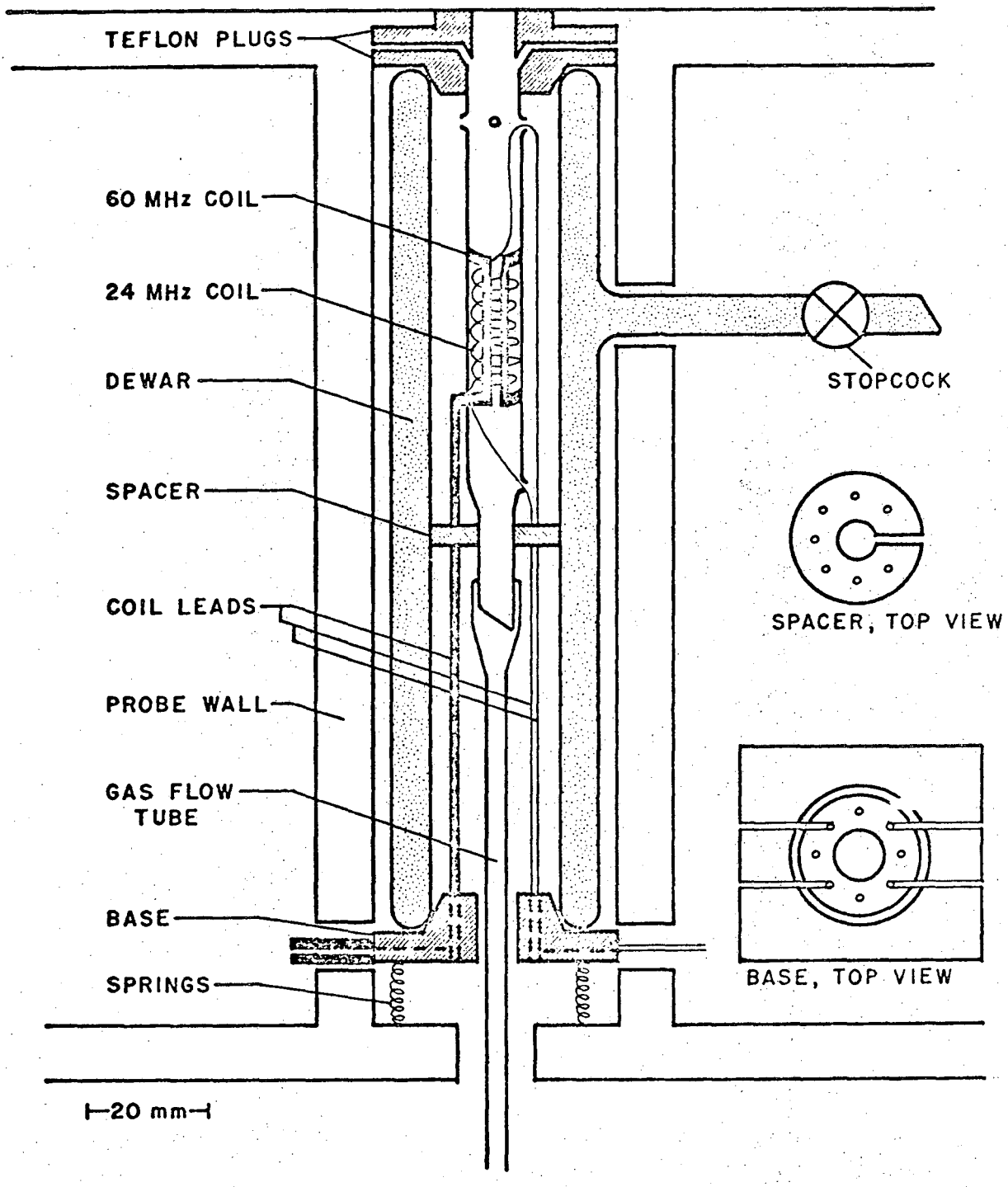

XBL7511-8743

Kohler et al.

FIGURE 3 JCP

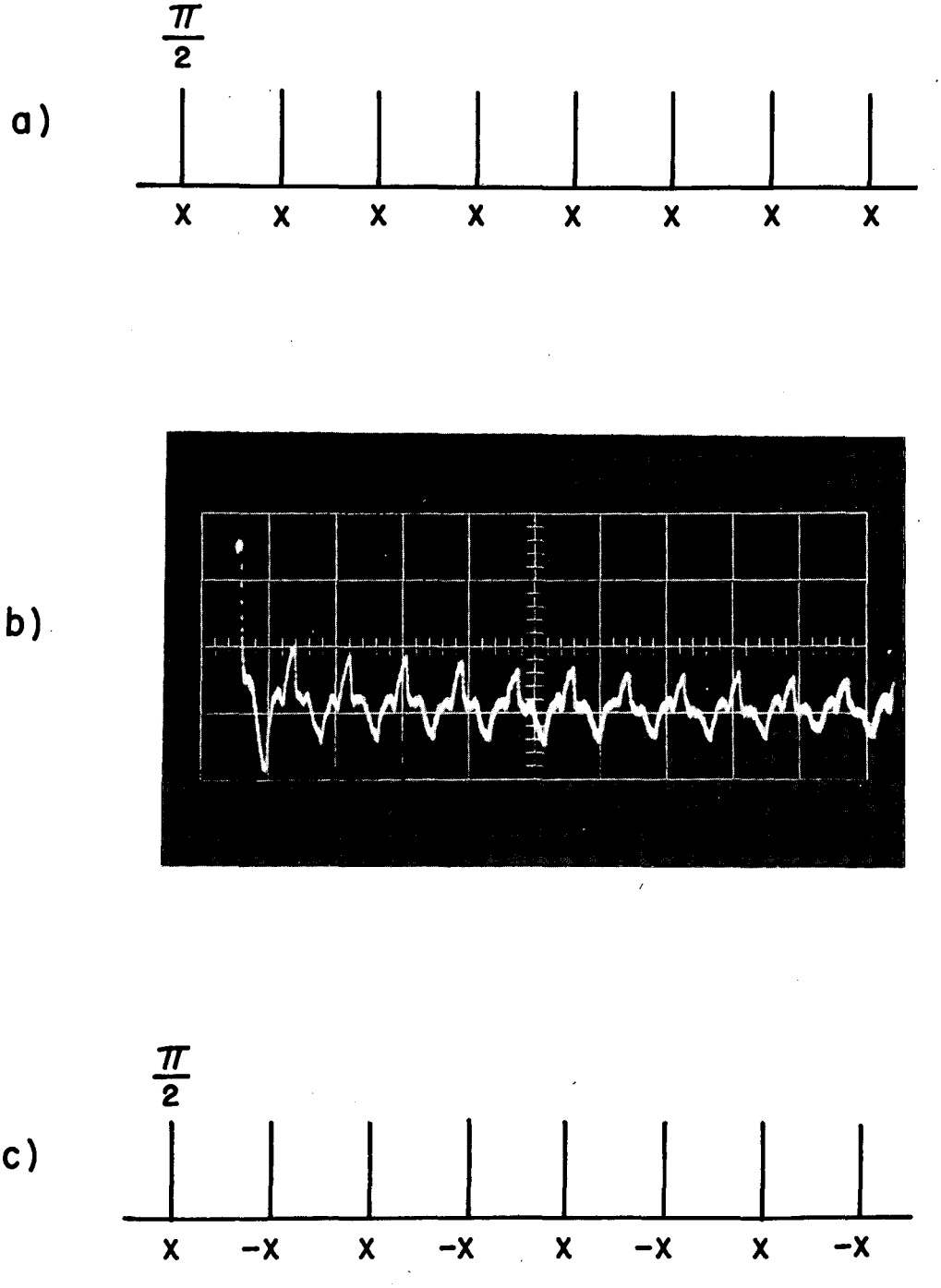

XBB 754-3166

Fig. 4

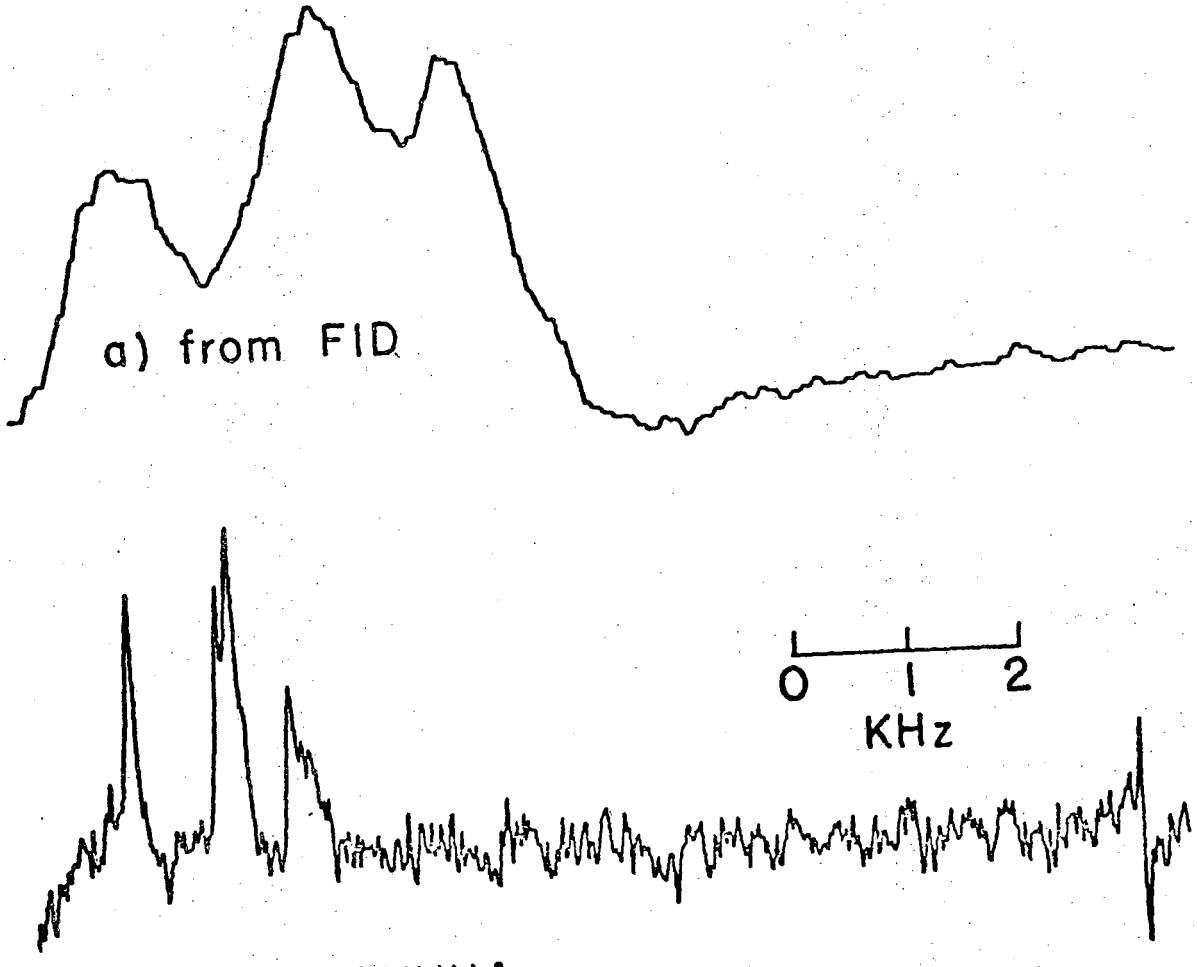

XBL756-5285

Kohler et. al.

FIG 5

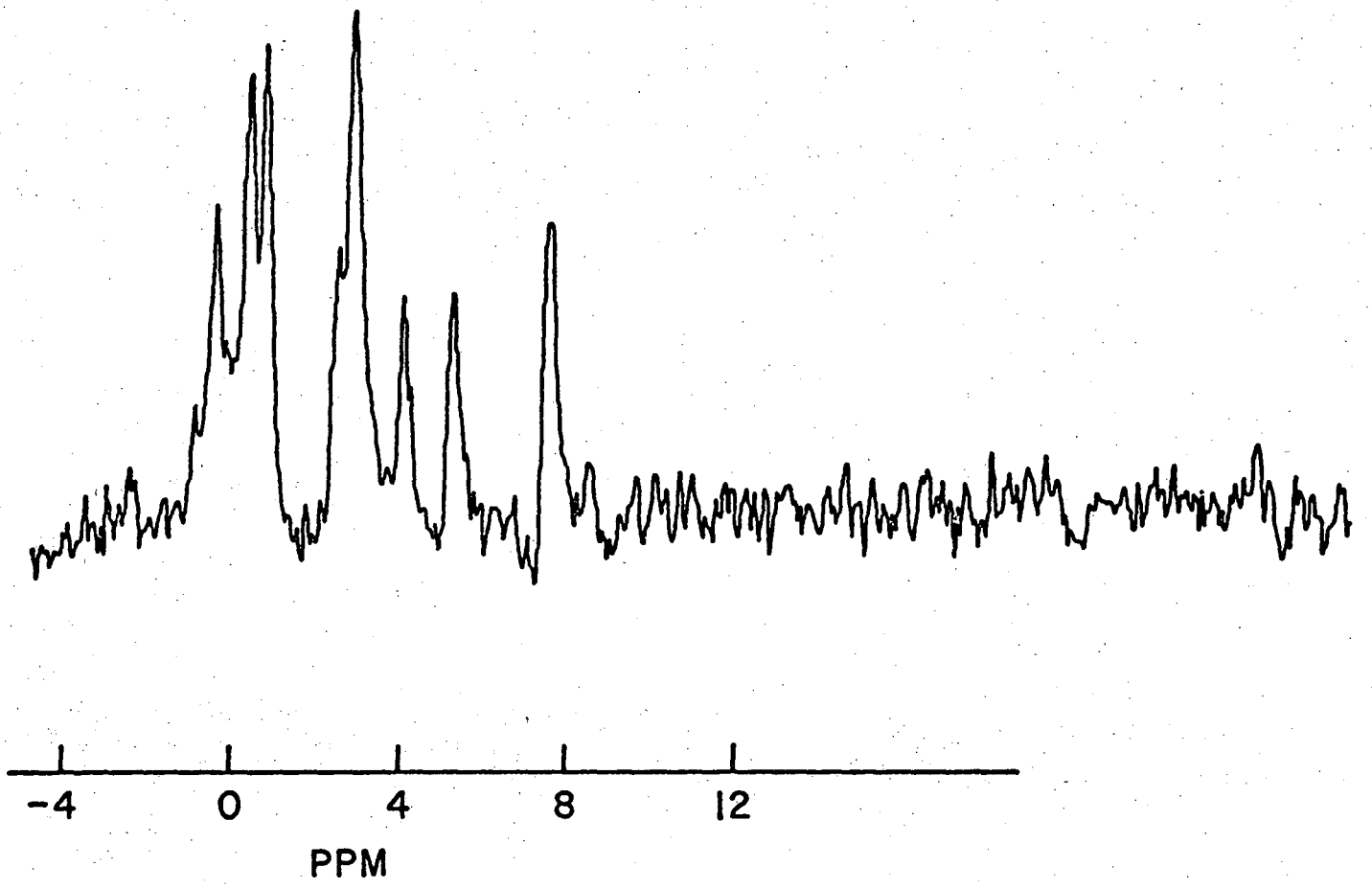

XBL756-5280

Kohler et al.

FIGURE 6 JCP

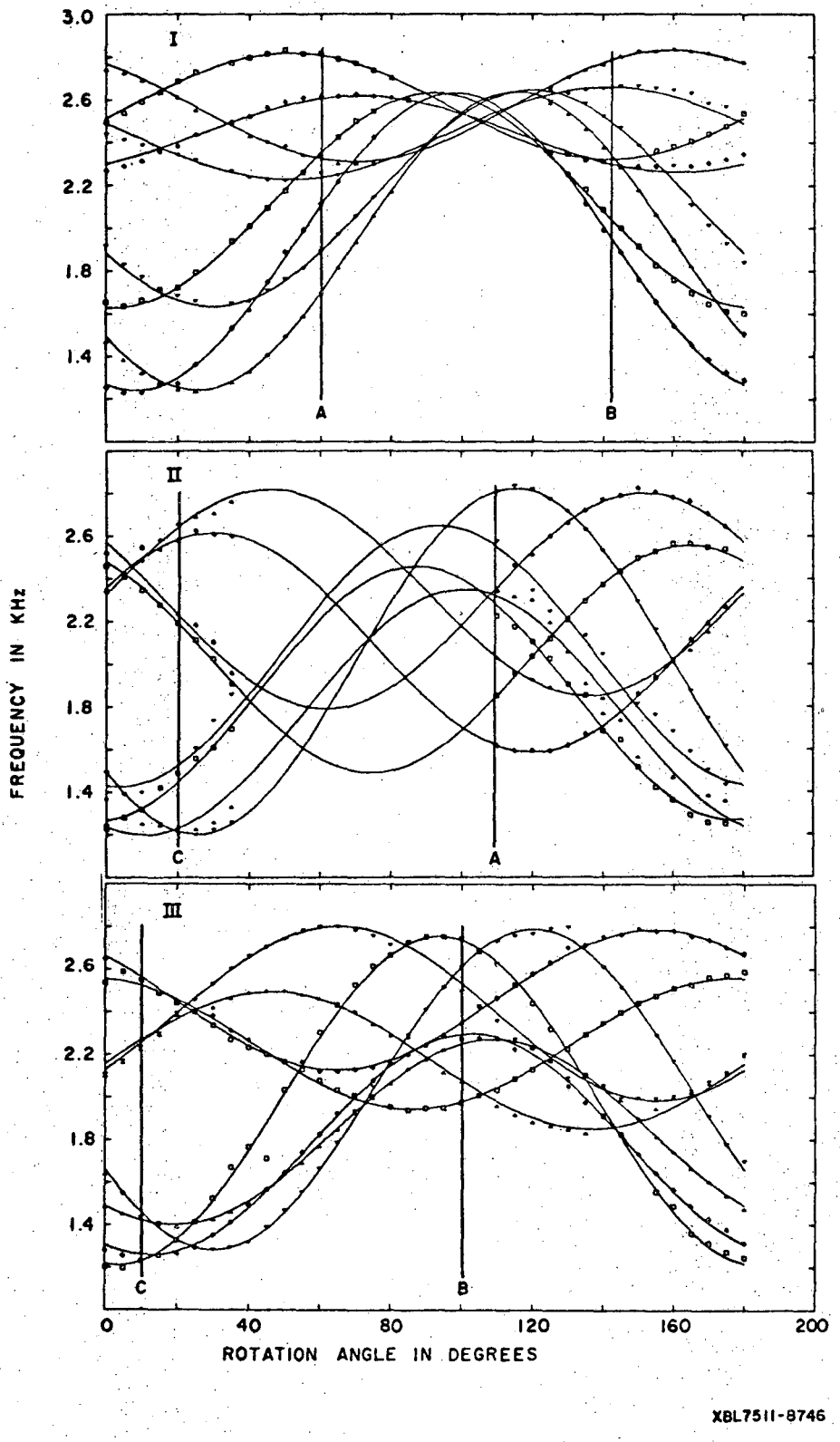

Kohler et al.

FIGURE 7 JCP

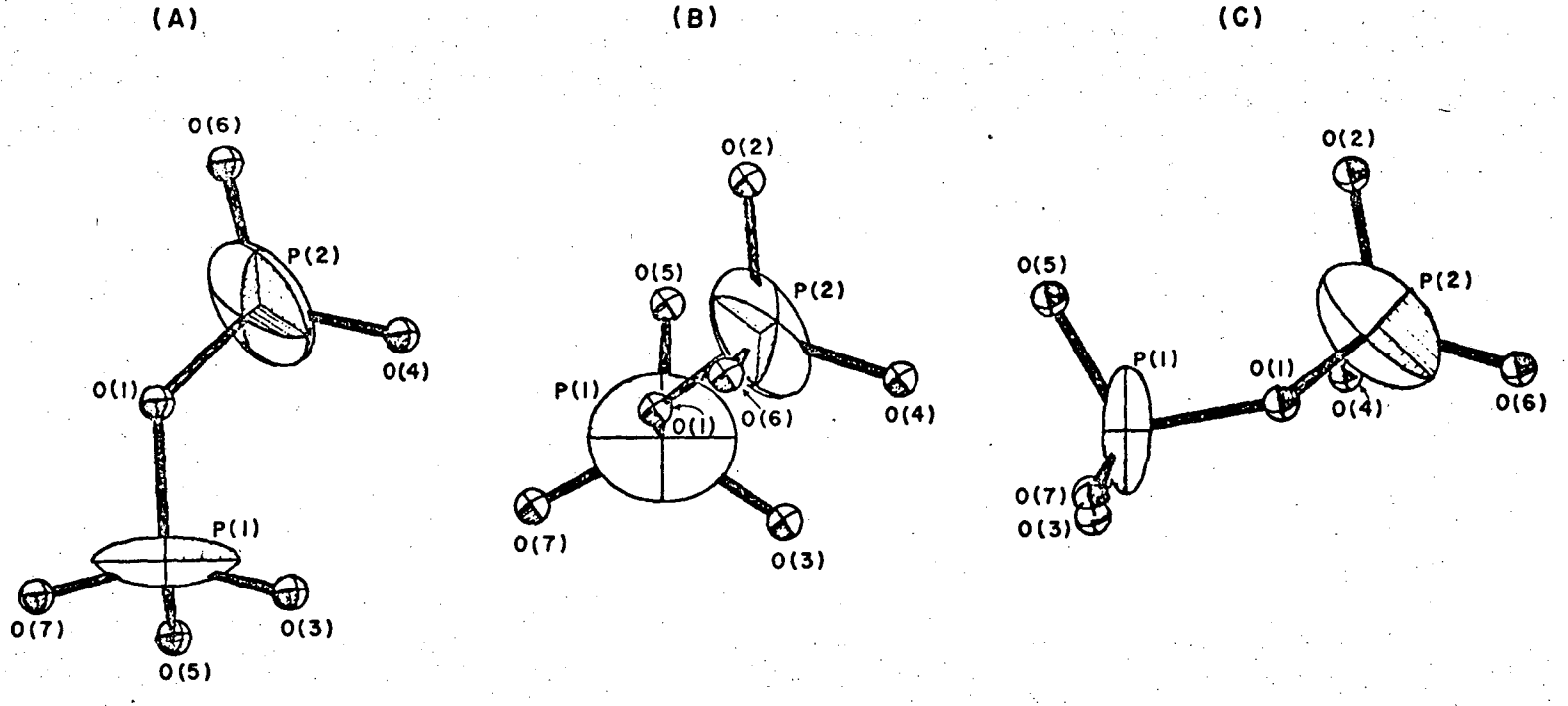

XBL7511-8744

JCP (2 col)

Kohler et al.

FIGURE 8

TECHNICAL INFORMATION DIVISION
LAWRENCE BERKELEY LABORATORY
UNIVERSITY OF CALIFORNIA
BERKELEY, CALIFORNIA 94720